Neurobiology of Stress 22 (2023) 100513

Contents lists available at ScienceDirect

Neurobiology of Stress

journal homepage: www.elsevier.com/locate/ynstr

Proteomic analysis identifies Stomatin as a biological marker for psychological stress

Yuan Cao [a,b,1], Si-Qi Ying [a,1], Xin-Yu Qiu [a,c], Jia Guo [a,b], Chen Chen [d], Shi-Jie Li [a,c], Geng Dou [a], Chen-Xi Zheng [a], Da Chen [a,b], Ji-Yu Qiu [a,e], Yan Jin [a,f,*], Bing-Dong Sui [a,**], Fang Jin [a,b,***]

[a] State Key Laboratory of Military Stomatology, National Clinical Research Center for Oral Diseases, Shaanxi International Joint Research Center for Oral Diseases, Center for Tissue Engineering, School of Stomatology, The Fourth Military Medical University, Xi'an, Shaanxi, 710032, China
[b] Department of Orthodontics, School of Stomatology, The Fourth Military Medical University, Xi'an, Shaanxi, 710032, China
[c] Department of Preventive Dentistry, School of Stomatology, The Fourth Military Medical University, Xi'an, Shaanxi, 710032, China
[d] Military Medical Psychology School, The Fourth Military Medical University, Xi'an, Shaanxi, 710032, China
[e] Department of VIP Dental Care, School of Stomatology, The Fourth Military Medical University, Xi'an, Shaanxi, 710032, China
[f] Xi'an Institute of Tissue Engineering and Regenerative Medicine, Xi'an, Shaanxi, 710032, China

ARTICLE INFO

Keywords:
Psychological stress
Extracellular vesicles
Proteomic analysis
Stomatin
Plasma

ABSTRACT

Psychological stress emerges to be a common health burden in the current society for its highly related risk of mental and physical disease outcomes. However, how the quickly-adaptive stress response process connects to the long-observed organismal alterations still remains unclear. Here, we investigated the profile of circulatory extracellular vesicles (EVs) after acute stress (AS) of restraint mice by phenotypic and proteomic analyses. We surprisingly discovered that AS-EVs demonstrated significant changes in size distribution and plasma concentration compared to control group (CN) EVs. AS-EVs were further characterized by various differentially expressed proteins (DEPs) closely associated with biological, metabolic and immune regulations and were functionally important in potentially underlying multiple diseases. Notably, we first identified the lipid raft protein Stomatin as an essential biomarker expressed on the surface of AS-EVs. These findings collectively reveal that EVs are a significant function-related liquid biopsy indicator that mediate circulation alterations impinged by psychological stress, while also supporting the idea that psychological stress-associated EV-stomatin can be used as a biomarker for potentially predicting acute stress responses and monitoring psychological status. Our study will pave an avenue for implementing routine plasma EV-based theranostics in the clinic.

1. Introduction

Emotional, physical, and environmental stressors represent dominant challenges of daily living (Labuschagne et al. 2019). In particular, psychological stress emerges to cause mental and physical health issues in modern society (Qin et al. 2014; Sandi and Haller 2015). While chronic exposures can lead to negative psychiatric consequences, acute stress is important for high prevalence and thought to be adapted quickly (Cai et al. 2017; Ji et al. 2022). According to the current knowledge, after exposed to psychological stress, physiological changes are fundamentally orchestrated by the sympathetic nervous system (SNS) and the hypothalamic-pituitary-adrenal (HPA) axis (Barel et al. 2018; Marques-Feixa et al. 2022). Each of these systems involves a quick adaptive response, within minutes or hours, to prepare the body to deal with the stressor encountered and return the body to a homeostatic state once the stressor has gone (Marques-Feixa et al. 2022; Sapolsky et al. 2000; Segerstrom and Miller 2004; Turner et al. 2020). In contrast to physiological adaptations, this quickly-adaptive response may also lead to consequences in pathological states (Hu et al. 2022; Obrist 1976). Previous systematic analyses of this issue have proposed that acute physiological stress reactivity predicts greater illness frequency in the future development of not only cognitive inability, depression and

* Corresponding author. State Key Laboratory of Military Stomatology & National Clinical Research Center for Oral Diseases & Shaanxi International Joint Research Center for Oral Diseases, Center for Tissue Engineering, School of Stomatology, The Fourth Military Medical University, Xi'an, Shaanxi 710032, China.
** Corresponding author.
*** Corresponding author. Department of Orthodontics, School of Stomatology, The Fourth Military Medical University, Xi'an, Shaanxi, 710032, China.
E-mail addresses: yanjin@fmmu.edu.cn (Y. Jin), bingdong@fmmu.edu.cn (B.-D. Sui), jinfang@fmmu.edu.cn (F. Jin).
[1] These authors contributed equally to this work.

https://doi.org/10.1016/j.ynstr.2023.100513
Received 7 August 2022; Received in revised form 24 December 2022; Accepted 2 January 2023
Available online 2 January 2023

anxiety, but also obesity, immune disorders, lower bone mass, and physical disability (Turner et al. 2020). Among these, significant findings have also indicated that acute physiological stress was related to a greater risk of cardiovascular disease (Carroll 2017) and decreased telomere length at follow-up (Shakirov et al. 2022). However, the detailed mechanisms underlying the quickly-adaptive response and its potential health impacts have not been fully elucidated.

For decades, with many researchers worldwide committing copious time and resources to characterize extracellular vesicles (EVs), scientists and clinicians have increasingly found that these small particles can escape from the autophagy-lysosomal pathway and play their roles in the extracellular space and circulation (Eden and Futter 2021; Maugeri et al. 2019). Whether EVs evoked by acute stress relates to potential disease outcomes or not has been interesting yet not understood. EVs are lipid-bound vesicles, containing nucleic acids and proteins, being released by cells to reach their targets (Doyle and Wang 2019). By transmitting multiple biological molecules, EVs are indispensable in mediating intercellular communications (Pegtel and Gould 2019; Pluchino and Smith 2019). Further notably, in response to a variety of pathological challenges, such as injury, infection, and stress, the characterization and function of circulating EVs are dramatically altered, which may be useful as both sensitive diagnostic biomarkers and contribute to the organismal regulation (Beninson and Fleshner 2014). Particularly, we have previously reported that chronic depression induces microRNA responses in local bone EVs to disrupt bone homeostasis (Hu et al. 2022). However, whether circulating EVs and their specific epitopes are influenced by psychological stress and can be identified for theranostic purposes remain unveiled (Bjørnetrø et al. 2019; Huang et al. 2015; Tan et al. 2017; Zeng et al. 2019).

In this study, we aimed to investigate whether plasma EVs responding to acute psychological stress, are associated with functional regulations and marked by specific surface markers. Taking advantage of a well-established restraint stress mouse model and standard and proteomic analyses of EVs, we discovered that EVs are an important function-related circulatory indicator after acute psychological stress and identified Stomatin expressed on EV surface as a biomarker for potentially predicting acute stress responses. Our findings will be helpful to understand the EV-mediated stress responses and to establish EV-mediated stress theranostics in the clinic.

2. Materials and methods

2.1. Animals

C57BL/6 female mice were used in this study and were purchased from the Laboratory Animal Center of the Fourth Military Medical University. All animal experimental procedures were approved by the Fourth Military Medical University and were performed according to the Guidelines of Intramural Animal Use and Care Committee of the Fourth Military Medical University. Mice were group-housed and maintained under specific pathogen-free conditions with standard 12 h light/dark cycles, and were kept feeding and drinking ad libitum.

2.2. Physical restraint model of acute stress

Mice were subjected to physical restraint by being held horizontally in 50-mL conical tubes with ventilating holes for a 12-h (10:00 p.m. - 10:00 a.m.) period, which is a well-established model for inducing psychological acute stress (AS) in mice (Hu et al. 2014; Pyter et al. 2014; Zhang et al. 2008). In this procedure, mice were not compressed and can move slightly forward and backward. Non-stressed control (CN) mice remained in home cages without food and water for the same period. Mice with only food and water deprivation (FWD) during the same period (10:00 p.m. - 10:00 a.m.) were also set as an experimental control. Immediately after the restraint period, mice were used to perform different behavior tests. Different behavior tests used different batches of mice. Besides, immediately (for most experiments) or at determined time points (for time-course experiments) after the restraint period, mice were sacrificed by cervical dislocation, and the plasma of the mice was collected to perform further experiments.

2.3. Open field test (OFT)

A black behavior test box (60 cm × 60 cm × 30 cm, length × width × height) was virtually divided into a center field and a periphery field. For each test, the mouse was placed in the periphery field, and the locomotion of the animal was recorded with a video camera for 15 min to measure the distance in the center or peripheral area (Sandi and Haller 2015). Each group had 12 mice according to previous reports (Pyter et al. 2014; Zhang et al. 2008) showing the requirements for behavioral tests, and the experiments were performed immediately after the restraint stress. The data were analyzed with JLBehv-LAM (Ecgonline, China).

2.4. Elevated plus maze test (EPMT)

A crossed maze with two closed and two open arms was applied and was elevated 30 cm above the ground. The mouse was placed at the end of the open arm. The locomotion of the animal was recorded with a video camera for 5 min (Sandi and Haller 2015). Each group had 12 mice according to previous reports (Pyter et al. 2014; Zhang et al. 2008) showing the requirements for behavioral tests, and the experiments were performed immediately after the restraint stress. The data were analyzed with JLBehv-EPMM (Ecgonline, China).

2.5. Enzyme-linked immunosorbent assay (ELISA)

Plasma was immediately collected from the whole blood from the retro-orbital venous plexus and stored at −80 °C until use. Corticosterone and norepinephrine concentrations were measured using ELISA kits (D721183, Sangon Biotech, China; ABN-KA1877, Abnova, China) according to the manufacturer's instructions. Each group had 6 mice for the determining of difference between groups in ELISA.

2.6. Isolation of plasma EVs

Plasma was collected and centrifuged at 3500 rpm for 15 min to remove the debris. The supernatant was further centrifuged at 2500 g for 10 min to remove the blood platelets(Coumans et al. 2017), which may influence the purity of EVs, after diluted with the same volume of phosphate buffer saline (PBS). The supernatant was further centrifuged at 16,500 g for 30 min to pellet the EVs (Tabletop High-Speed Micro Centrifuges, CT15E, Hitachi, Japan). The pellet was then resuspended with 0.2 μm-filtered PBS for subsequent experiments.

2.7. Transmission electron microscopy (TEM)

The morphology of the isolated EVs was determined by TEM (TECNAI Spirit, FEI, USA), as stated previously(Zheng et al. 2021). A total of 4 μL of the EV solution at a protein concentration of 1 mg/ml was deposited onto a carbon-coated 400-square mesh copper grid. Ten minutes after the sample was deposited, the grid was rinsed with 10 drops of deionized water. A drop of 1% phosphotungstic acid (12501-23-4, RHAWN, China) was added to the grid to conduct the negative staining. The grid was subsequently dried naturally and visualized using the 120-kV FEI TEM. TEM-EDS was conducted using a field emission TEM (JEOL, Japan).

2.8. Nanoparticle tracking analysis (NTA)

The size distribution and concentration of the isolated EVs were analyzed by the Nanosight NS300 system (Malvern Panalytical, UK), as

stated previously(Zheng et al. 2021). Briefly, EVs were diluted 1:1000 in PBS. Each sample analysis was conducted for 60 s. Data were analyzed by Nanosight NTA 2.3 Analytical Software with the detection threshold optimized for each sample and screen gain at 10 to track as many particles as possible with the minimal background. A blank 0.2 μm-filtered PBS was also run as a negative control. Each group had 6 mice for the determining of difference between groups in NTA. At least 3 repeats were done for each sample.

2.9. Western blot (WB) analysis

The isolated EV proteins were extracted using the RIPA lysis buffer (P0013B, Beyotime, China). The protein concentration was determined by the BCA protein assay kit (PA115, TIANGEN, China). All samples were prepared at a final concentration of 1 μg/μl in loading buffer (CW0027S, CwBio, China). Protein samples (20 μg) were loaded into a 4–20% SDS-polyacrylamide gel (LK206, Epizyme, USA) in the Bio-Rad Electrophoresis System to separate the proteins with different molecular weights. The proteins in the gel were then transferred to polyvinylidene difluoride (PVDF) membranes. After blocking in 5% bovine serum albumin (BSA) solution (218072801, MP Biomedical, USA), the membranes were incubated with primary antibodies (CD63, SC5275, Santa Cruz Biotechnology, USA; Caveolin-1, sc53564, Santa Cruz Biotechnology, USA; Flotilin-1, PTM-5369, PTM BIO, China; Golgin-84, nbp1-83352, Novus Biologicals, USA; β-actin, CW0096M, Cwbio, China; Stomatin, ab166623, Abcam, UK; Me1, 16619-1-AP, Proteintech, China; Adh1, A19624, ABclonal, China; Igfbp3, 10189-2-AP, Proteintech, China; Fap, NBP2-89135, Novus Biologicals, USA; diluted all at 1:1000) at 4 °C overnight. After incubation with the corresponding secondary antibodies (111-035-003, Jackson ImmunoResearch, USA), the PVDF membranes were imaged using Western chemiluminescent horseradish peroxidase (HRP) substrate (Millipore, USA) with an imaging system (Tanon 4600, Shanghai, China). The original uncropped images were uploaded as Supplementary Materials.

2.10. Proteomic analysis

Protein lysates of plasma EVs in the CN and AS groups were prepared and subjected to LC-MS/MS analysis(Zheng et al. 2021) on an Orbitrap Exploris™ 480 mass spectrometer with a NanoSpray III ion source. The raw data was analyzed using Proteome Discoverer system (v2.4.1.15). Proteins were identified by comparing with the Uniport database with a false discovery rate set at 0.01 for both peptides and proteins. Proteins were quantified using the default parameters in MaxQuant. Among the identified proteins, 154 proteins were differentially expressed proteins (DEPs) (fold change>1.5 and p value < 0.05). Proteins were included for further functional analysis based on Gene Ontology (GO) and Kyoto Encyclopedia of Genes and Genomes (KEGG) databases. The DEPs (Table S1) and the full data (Table S2) were uploaded as Supplementary Material.

2.11. GO analysis

GO annotation of the proteome was derived from the UniProt-GOA database (http://www.ebi.ac.uk/GOA/). Firstly, identified protein ID was converted to UniProt ID and was then mapped to GO IDs by protein ID. If identified proteins were not annotated by UniProt-GOA database, the InterProScan soft was used to annotate protein's GO function based on protein sequence alignment method. Then proteins were classified by GO annotation based on three categories: biological process, cellular component, and molecular function.

2.12. KEGG analysis

KEGG Pathways mainly including: Metabolism, Genetic Information Processing, Environmental Information Processing, Cellular Processes, Organismal Systems, Human Diseases and Drug development. KEGG database was used to annotate the protein pathway. Firstly, the KEGG online service tool KAAS was used to annotate protein's KEGG database description. Then the annotation results were mapped on the KEGG pathway database using the KEGG online service tool KEGG mapper.

2.13. Flow cytometry (FCM) analysis

The isolated EVs were stained with the membrane dye (CellMask, C10045, Invitrogen, USA, diluted at 1:3000) for 37 °C, 5 min, and stained with the primary antibody (Stomatin, ab166623, Abcam, UK, diluted at 1:100) for 2 h at 4 °C. After washing with PBS, EVs were subsequently incubated with the corresponding secondary antibody (A16024, Invitrogen, USA, diluted at 1:500) on the ice for 1 h in the dark. The percentages of positively stained EVs were determined with a flow cytometer (NovoCyte; ACEA Biosciences, USA) and analyzed using NovoExpress software, as stated previously (Zheng et al. 2021).

2.14. Immunofluorescence (IF) staining

The isolated EVs were marked with the membrane dye (CellMask, C10045, Invitrogen, USA, diluted at 1:3000) for 37 °C, 5 min, and stained with the primary antibody (Stomatin, ab166623, Abcam, UK, diluted at 1:100) at 4 °C overnight. After washing with PBS, EVs were incubated with the appropriate fluorescence-conjugated antibody (A16024, Invitrogen, USA, diluted at 1:500) at 4 °C for 1 h in the dark. The EVs were imaged by the confocal microscope (A1plus, Nikon, Japan) on dropping onto coverslips. Three images were captured per slide.

2.15. Statistic analysis

All data were expressed as mean ± standard deviation (SD). Statistical comparisons between data sets were made with an analysis of normality and variance, followed by a two-tailed unpaired Student's *t*-test for comparing differences between two groups and a one-way ANOVA followed by post hoc tests for comparing differences among several groups. All statistical analysis was conducted using the GraphPad Prism 9.0.0 software. Differences were considered statistically significant when $p < 0.05$.

3. Results

3.1. Acute physical restraint induces psychological stress in mice

To investigate the potential effects of stress on circulatory EVs, we first established a standard laboratory model of acute psychological stress through tube restraint and performed standard behavioral and serological indicator tests (Hu et al. 2014). In the OFT (Fig. 1A), mice that suffered from 12 h immobilization showed a less complex path than the respective CN mice, which was confirmed by the statistical analysis showing reduced center distances of experimental mice in a 15-min test session (Fig. 1B, $p = 0.0003$). In the EPMT (Fig. 1C), the open arm time for mice exposed to the tube restraint was also decreased compared with the CN mice in a 5-min test session (Fig. 1D, $p = 0.0184$). Because the CN mice were undergoing FWD for 12 h, to compare the potential stress of CN mice with the normal mice, we also analyzed their behaviors. As shown in Fig. S1, we tested FWD mice and the normal mice (denoted as CN of this experiment) in the OFT and EPMT, these two groups of mice showed no significant difference from each other (Figs. S1A–D). Furthermore, serological tests of corticosterone and norepinephrine levels demonstrated that the recognized behavioral changes were accompanied by physiological alternations after AS. As shown, the plasma corticosterone concentration was higher in the AS group than in the CN group (Fig. 1E, $p = 0.0080$), with a higher plasma norepinephrine level as well (Fig. 1F, $p = 0.0068$). Results above collectively

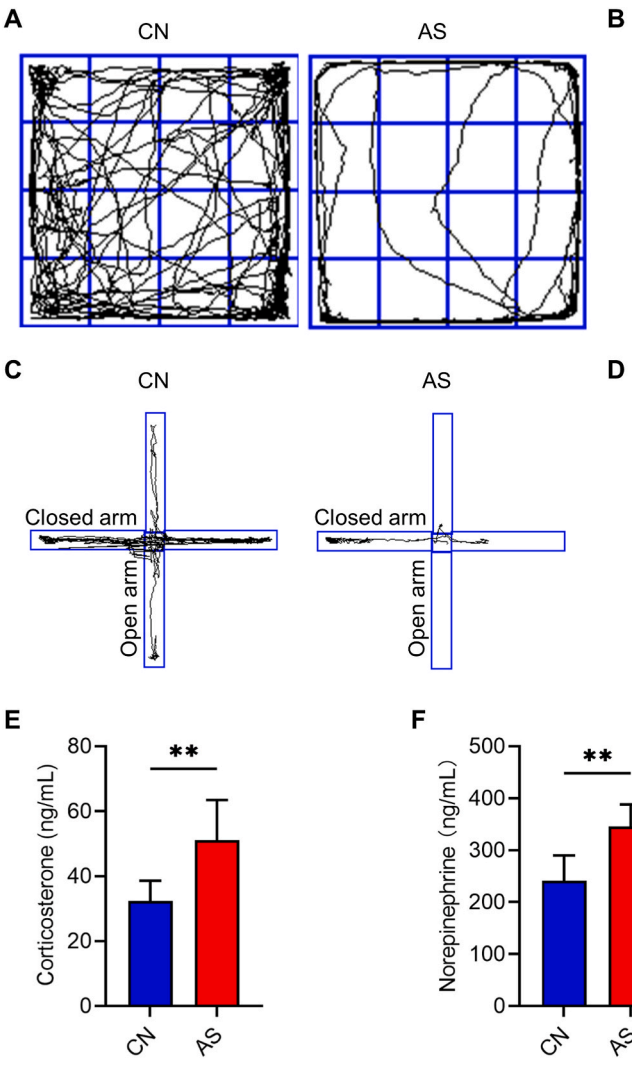

Fig. 1. Establishment of acute psychological stress in mice. (**A**) Tracing of locomotion for the respective control (CN) and acute stress (AS) mice in the open field test (OFT). AS mice after being restrained in tubes for 12 h showed reduced mobility and were less inclined to the center of the field. The corresponding quantitative graph is shown to the right. (**B**) Quantification of center distances during the OFT. (**C**) Locomotion traces for the representative CN and AS mice in the elevated plus maze test (EPMT). Closed arms are the horizontal lines and open arms are the vertical lines. (**D**) Quantification of open arm times during the EPMT. $N = 12$ mice for each group. (**E**) The plasma corticosterone levels of the CN and AS groups were quantified by ELISA. (**F**) The plasma norepinephrine level in each group was quantified by ELISA. $N = 6$ mice for each group. Data are presented as mean ± standard deviation (SD). *p < 0.05, **p < 0.01, two-sided unpaired *t*-test.

suggested acute restraint induces psychological stress in mice.

3.2. AS induced phenotypic alterations of plasma EVs

Next, we investigated whether acute psychological stress provoked plasma EV changes. As a representative of the easy-isolated EV population, the large EV riched fractions were purified from the peripheral blood of the AS mice and the CN mice using an established protocol of serial differential centrifugation (Coumans et al. 2017). We found that the acute stress extracellular vesicles (AS-EVs) of the time immediately after stress (0 h) were characterized by lower plasma concentration than the control group extracellular vesicles (CN-EVs) (Fig. 2A, p = 0.0002), which increased over time. At 8 h after stress, AS-EVs showed no difference from the CN-EVs (Fig. 2A). The size difference was further verified by NTA, the results of which showed the median size of the AS-EVs at 0 h was larger than the median size of CN-EVs (Fig. 2B, p = 0.0025). This effect also diminished over the time course and was not significant at 4 h (Fig. 2B). We thus performed the following analysis on AS-EVs at 0 h. After counting the particle numbers throughout different size distributions of CN-EVs and AS-EVs, the AS-EVs were revealed to have a greater amount of particles in sizes at 250 nm and 300 nm than the CN-EVs, while smaller amount of particles in sizes at 50 nm and 100 nm, which indicated a tendency toward a larger sized population of EVs upon AS (Fig. 2C). Using TEM, we found EVs of both groups were "cup-shaped" with sizes of most particles ranging from 100 nm to 200 nm, between which the AS-EVs were potentially larger (Fig. 2D). Western blot then confirmed the expression of EV markers in both groups. The widely recognized proteins of EVs, such as the tetraspanin molecule CD63, the lipid raft protein Flotillin-1 and the integrated plasma membrane protein Caveolin-1, were all detectable in CN- and AS-EVs, whereas the Golgi integral membrane protein Golgin-84 was negative (Fig. 2E). Taken together, both CN- and AS-EVs are confirmed in this study, while AS-EVs are phenotypically altered.

3.3. Proteomic profiling identified differentially expressed proteins between CN-EVs and AS-EVs

Next, we examined whether acute psychological stress also induced protein content alterations in EVs. Paired CN-EVs and AS-EVs samples were analyzed using high-resolution mass spectrometry, which identified 154 differentially expressed proteins (DEPs) (Table S1) in CN- and AS-EVs, among which 76 DEPs were significantly down-regulated in AS-EVs and 78 DEPs were significantly up-regulated (Fig. 3A and B). The verification of the top five proteins of DEPs was shown (Fig. S2A). We next characterized the identified DEPs regarding their subcellular localization. Most of the DEPs (50.65%) were consistent with the extracellular distribution, while over 20.13% DEPs originated from the cytoplasm (Fig. 3C). Plasma membrane (2.6%), organelle (endoplasmic reticulum, 2.6%, and mitochondria, 9.74%) and nucleus (over 7.14%) proteins were also identified in the differentially expressed proteome

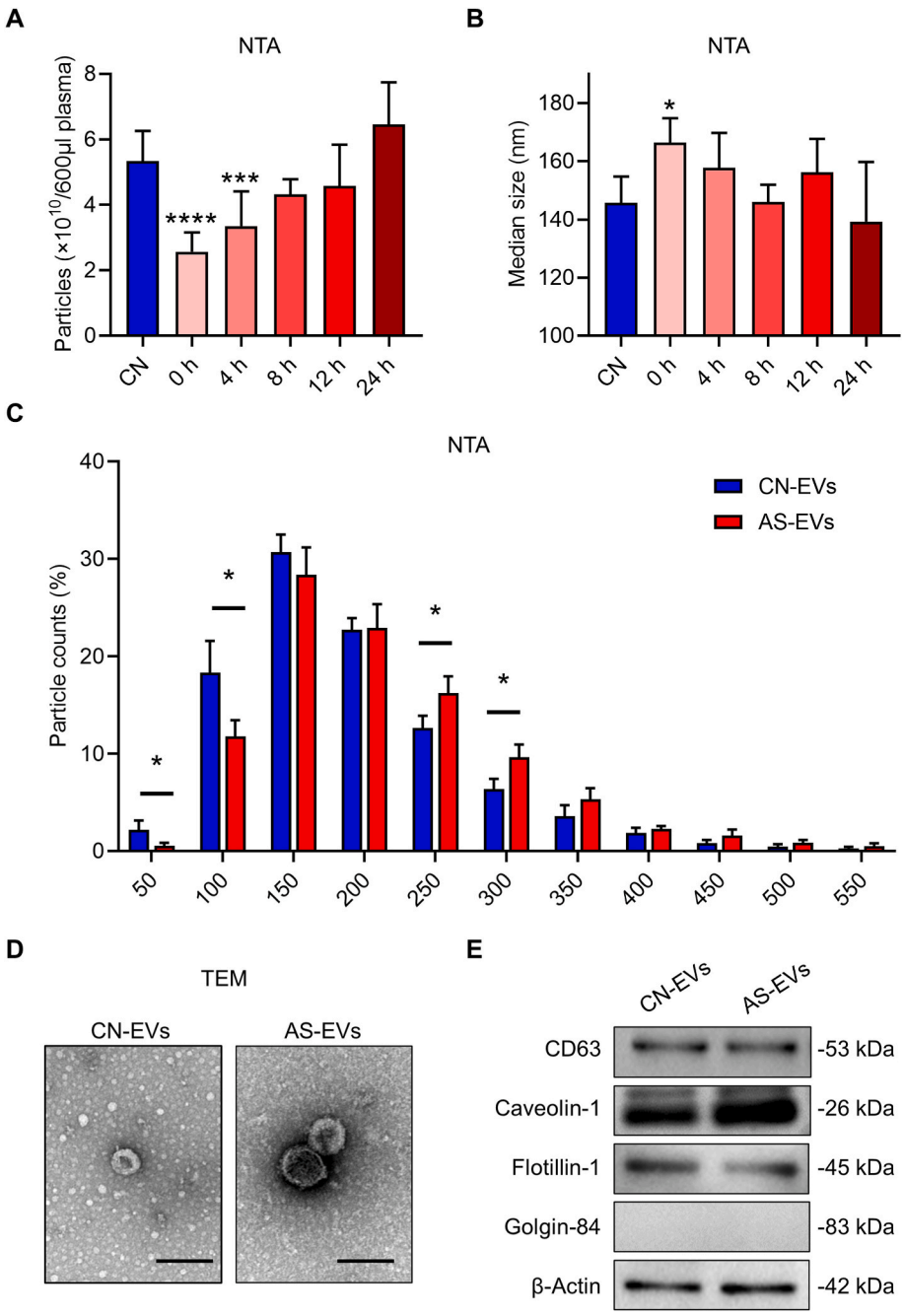

Fig. 2. Phenotypic characterization of CN and AS-induced plasma EVs. (**A**) NTA demonstrated the concentration of CN-EVs and AS-EVs per 600 μL plasma over a 24-h time course. $N = 6$ mice for each group. (**B**) The median size of EVs of nanoparticle tracking analysis (NTA) showing AS-EVs and CN-EVs over a 24-h time course. $N = 6$ mice for each group. (**C**) The percentages of EVs ranging from different size distributions were determined by NTA in CN and AS groups immediately after stress. $N = 6$ mice for each group. (**D**) Transmission electron microscopy (TEM) graphs of plasma EVs from CN and AS mice. Bars: 200 nm. (**E**) Western blot analysis confirmed the presence of EV-marker CD63, Flotillin-1, and Caveolin-1 while being negative for the cell-marker, Golgi integral membrane protein Goglin-84. Data are presented as mean ± standard deviation (SD). *p < 0.05, **p < 0.01, two-sided unpaired *t*-test or one-way ANOVA followed by post hoc tests.

(Fig. 3C). Further GO analysis of the Biological Process suggested that the DEPs were stimuli responsive and biologically active, which in particular potentially regulated the metabolic and immune function (Fig. 3D). GO analysis of the Molecular Function also indicated involvement of DEPs in binding, catalytic activity and molecular function regulation (Fig. 3D). These findings together revealed that EVs are adapted to stress in the protein content, which may correlate with functional regulations.

3.4. AS-EVs were characterized with functionally classified proteins

We then focused on these DEPs and carried out further functional enrichment analysis. Biological Process enrichment analysis suggested multiple detailed stress responses, metabolic and immune regulations were associated with AS-EVs, including the regulation of extracellular matrix organization, negative regulation of lipid localization, acute-phase response and regulation of innate immune response (Fig. 4A, red boxes). Additional information indicated AS-EVs were involved in oxidative and antioxidative regulations, as well as bacterial defense reactions, such as respective enrichment in hydrogen peroxide catabolic or metabolic processes and toll-like receptor signaling pathway, antibiotic catabolic process, pattern recognition receptor signaling pathway, response to bacterium and regulation of defense response (Fig. 4A, blue boxes). The enrichment in the regulation of secretion by cell confirmed the EV participation in AS (Fig. 4A). Regarding the Molecular Function, DEPs were especially enriched in protein tyrosine phosphatase activator activity, protein phosphatase activator activity, phosphatase activator activity, angiostatin binding, spectrin binding, metalloendopeptidase activity, insulin-like growth factor binding and fibronectin-binding, which were also corresponded to the Biological Process enrichment analysis results in extracellular matrix organization and biological regulation (Fig. 4B). Enrichment analysis in Cellular Components then

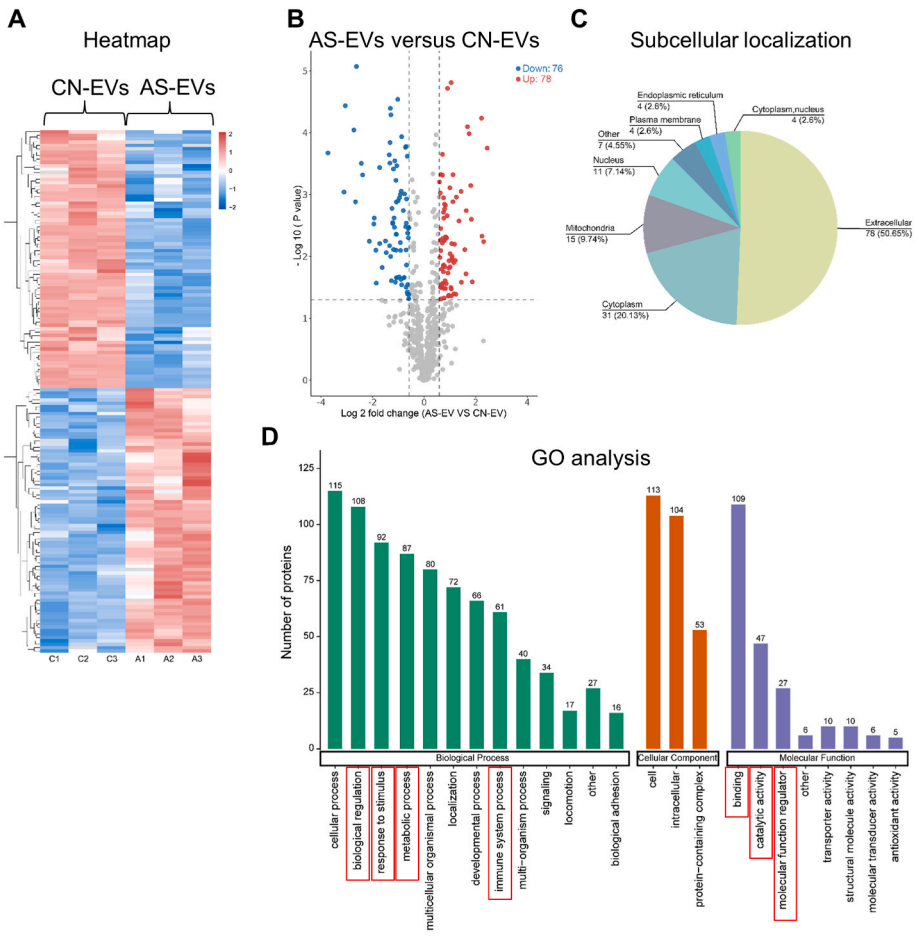

Fig. 3. Proteomic profiling of CN- and AS-EVs. (**A**) Hierarchical clustering of differentially expressed proteins (DEPs) (fold change >1.5 and P value < 0.05) between CN-EVs and AS-EVs, with protein abundance being normalized as the Z-score. Rows represent the DEPs and columns represent individual replicates. (**B**) Volcano plot showing significantly upregulated (red dots) and downregulated (blue dots) proteins in AS-EVs, compared to CN-EVs. (**C**) Distribution of the differentially expressed proteome in subcellular location categories retrieved from UniProt database according to Gene Ontology (GO) annotation. (**D**) GO analysis of total DEPs, categorized into 'Cellular component', 'Molecular function' and 'Biological process'. Red boxes indicate terms of interest. (For interpretation of the references to color in this figure legend, the reader is referred to the Web version of this article.)

identified detailed targets of proton-transporting two-sector ATPase complex, proton-transporting ATP synthase complex, insulin-like growth factor ternary complex and growth factor complex, suggesting energy-required cell proliferation regulation by EVs in response to AS (Fig. 4C, red boxes). Besides, multiple cellular membranous system components were enriched, including endolysosome membrane, anchored component of plasma membrane, endolysosome and endocytic vesicle lumen, which were potentially in relation to the EV generation and release processes (Fig. 4C, blue boxes).

To analyze the interrelationships among the DEPs, we further used the STRING network tool to construct a PPI network. Core genetic analysis of the PPI network was performed using the CytoHubba plugin in Cytoscape software and indicated close correlations among the DEPs (Fig. 4D). To further investigate the functions of DEPs in AS-EVs, we performed analyses according to the KEGG database categories. KEGG annotations were assigned to 34 classes, mainly related to cellular processes, human diseases and environmental information processing (Fig. 4E). Particularly, for human diseases, DEPs were associated with immunological (notably COVID-19, as well as systemic lupus erythematosus), metabolic (carbon metabolism and diabetic complications), injury (cardiomyopathy and alcoholic hepatology) and neurological (spinocerebellar ataxia and Huntington disease) disorders (Fig. 4E, red boxes). In other KEGG categories, functional regulations of DEPs were putatively involved in phagocytosis (EVs or bacterium), cytoskeleton changes, ECM-receptor interactions, and detailed metabolic and immune processes (Fig. 4E, blue boxes). Taken together, these results collectively highlighted the various complex functional adaptations of EVs to psychological stress.

3.5. Surface stomatin marked the AS-induced plasma EVs

The above results prompted us to further examine the surface epitopes of AS-EVs, which thus might play important roles as potential biomarkers of psychological stress and are related to functional predictions. Among the top five DEPs, alcohol dehydrogenase 1 (Adh1), malic enzyme 1 (Me1) and insulin like growth factor-binding protein 3 (Igfbp3), are putatively not surface proteins, despite their persistent changes after AS (Fig. S2A). Furthermore, of the top five DEPs potentially exposed on the EV surface, expression of fibroblast activation protein (Fap) at 0 h after AS was not apparently changed, despite delayed upregulation, and that the intensity of Stomatin (Stom) was higher than Fap by the proteomics data, although the Stomatin expression ratio in AS-EVs over CN-EVs did not outpass Fap (Fig. S2A). Indeed, as a lipid raft membrane protein, Stomatin as a potential indicator of the AS-EVs might be sensitive and can be easily detected, and we select Stomatin as the marker of interest. Then we further verified the expression of Stomatin using WB analysis (Fig. 5A; Fig. S2A). The AS-EVs indeed showed a higher level of Stomatin expression than the CN-EVs at 0 h after stress, by an average of 2.93 compared to 1.58 fold changes (Fig. 5A, $p = 0.048$). Moreover, the effect of the Stomatin lasted for at least 24 h (Fig. S2A). The PPI network of Stomatin performed by the MCODE plugin for module analysis also revealed that Stomatin was crucial among the core proteins in the fibronectin 1 (FN1) module, which potentially regulated membrane interactions (Figs. 4D and 5B). To further confirm the surface expression, FCM analysis was conducted, which demonstrated that Stomatin exposure increased from 7.04% in the CN-EVs to 23.66% in the AS-EVs (Fig. 5C, $p = 0.005$). The gating strategy and sample tests of the AS-EVs and CN-EVs using the FCM were additionally shown (Figs. S2B and S2C). IF staining technique was

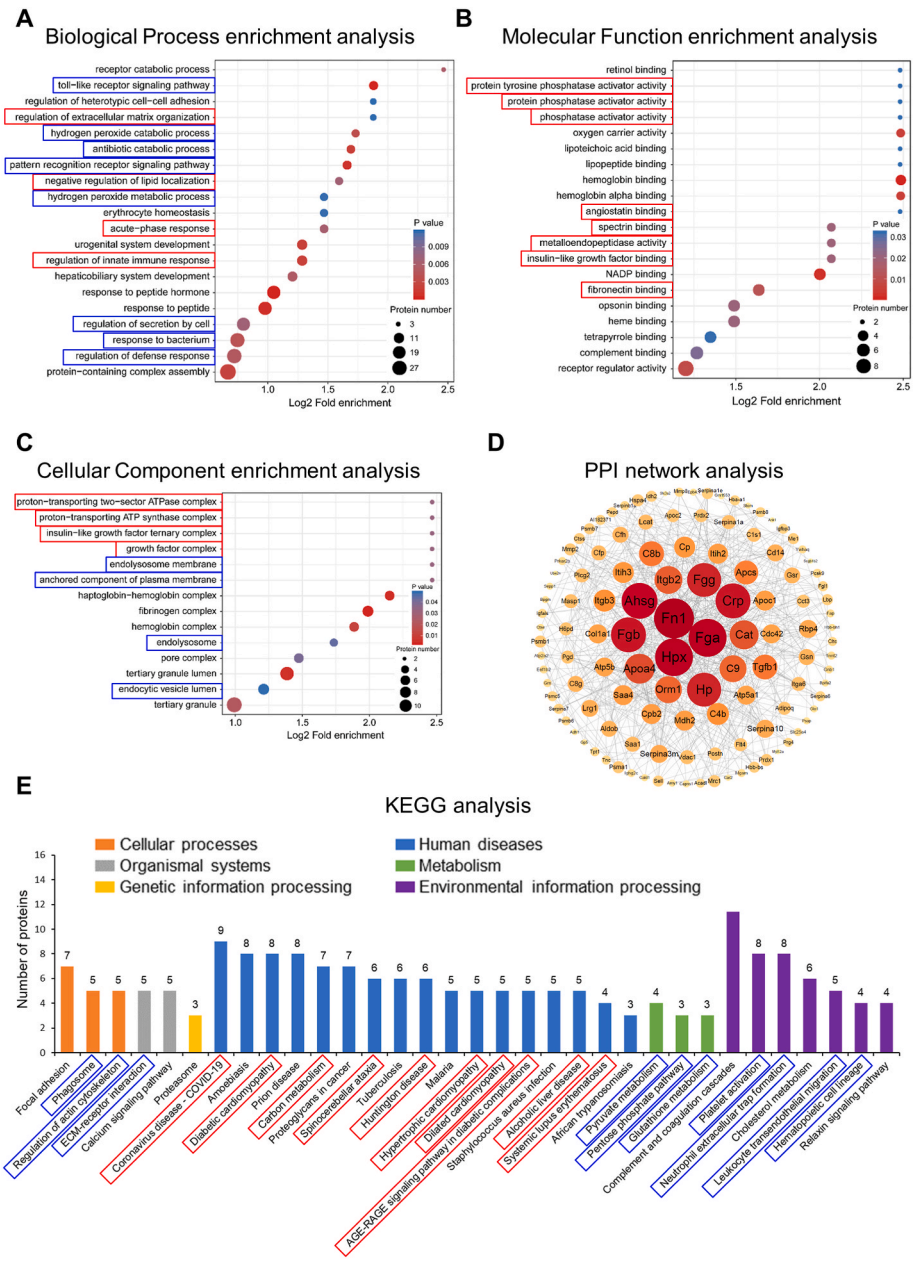

Fig. 4. Functional classification and enrichment analysis of CN- and AS-EVs. (**A-C**) GO enrichment analysis of total DEPs between CN-EVs and AS-EVs. The top twenty enriched terms of the 'Biological Process' categories (**A**), 'Molecular Function' categories (**B**), and 'Cellular Component' categories (**C**) were respectively presented as bubble charts. The Y-axis represents GO terms and the X-axis represents rich factors. The color of the bubble represents enrichment significance and the size of the bubble represents the number of DEPs. (**D**) Protein-protein interaction (PPI) network analysis of DEPs. (**E**) Kyoto Encyclopedia of Genes and Genomes (KEGG) pathway analysis of total DEPs. Red and blue boxes indicate terms of interest. (For interpretation of the references to color in this figure legend, the reader is referred to the Web version of this article.)

further used to directly observe the surface Stomatin of EVs, and Stomatin was indeed enriched in the AS-EVs (Fig. 5D). These findings suggested that surface Stomatin marked the AS-induced plasma EVs.

4. Discussion

Acute psychological stress represents a quite common health burden for people in the current society for its highly related risk of disease outcomes (Turner et al. 2020). However, the mechanism of this phenomenon has not been fully addressed. Particularly, whether and how the quickly-adaptive response connects with prolonged physical alterations is still unclear. EVs are biologically active intercellular communicators which are dynamic upon various pathological states (Eden and Futter 2021). In the present study, we demonstrated for the first time that under acute psychological stress, the phenotypic and proteomic profiles of circulating EVs are substantially altered. Data indicated that the stress effects on EV morphology were most apparent immediately after release of stress, but the protein content, particularly Stomatin expression, can be persistent over a 24-h period. We further identified Stomatin as a previously unrecognized surface biomarker of AS-EVs. Considering the small sample size in our experiments, we have performed different methods to verify the results, such as the Western blot, the flow cytometry and immunofluorescent staining. The findings were consistent in revealing a sensitive and stable biomarker expression, with potentially lasting effects. These findings will be useful for clinical assessing the psychological stress state and predicting the organismal functional changes.

Acute stress is known to be a risk factor for psychiatric disorders, and stress-induced animal models of emotional illness have been widely investigated (Li et al. 2017). Acute stress is also important in daily life for its high prevalence in modern society. Our study adopted the 12 h restraint model as an acute psychological paradigm to induce stress-like behaviors in mice, as previously reported (Pyter et al. 2014; Zhang et al. 2008). We behaviorally characterized this mouse model where we observed decreased exploratory activity in the OFT and decreased time spent in the open arm of the EPMT. In addition, increased corticosterone

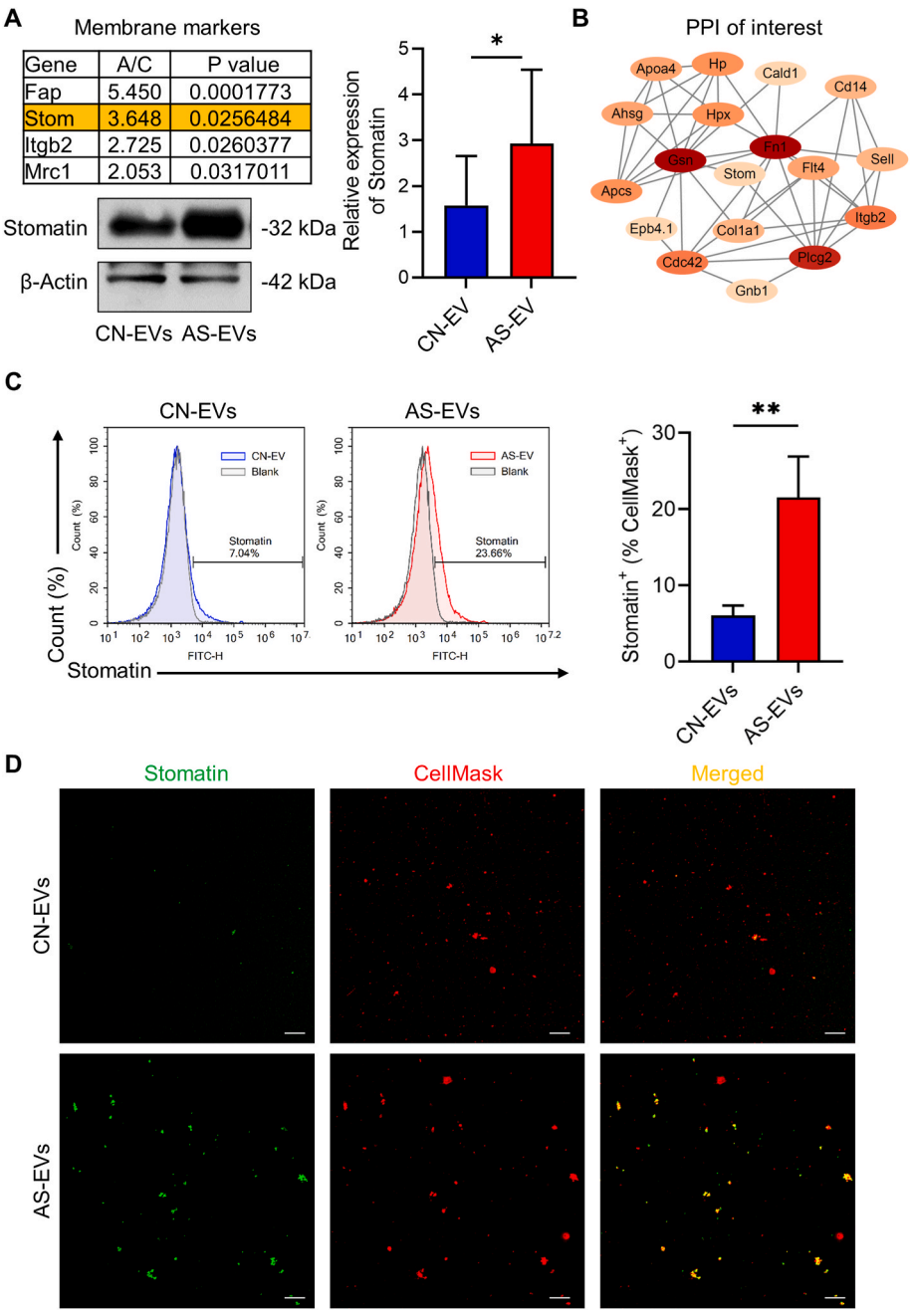

Fig. 5. Identification of Stomatin expressed on the surface of AS-EVs. (**A**) The AS-EVs over CN-EVs ratio and the P-value of identified membrane proteins were shown in the table (fold change >2.0). Western blot analysis and quantification confirmed the high expression of Stomatin in AS-EVs. (**B**) PPI network analysis of DEPs of interest. Stomatin (Stom) was demonstrated with close relationships with other DEPs. (**C**) Flow cytometric analysis showed Stomatin expression on the surface of EVs, with a higher percentage of surface Stomatin on AS-EVs than CN-EVs. The CellMask membrane dye was used to distinguish EVs from all particles and the blank samples indicate experimental controls. (**D**) Representative immunofluorescent (IF) staining images of Stomatin on EVs, which are counterstained by the CellMask membrane dye (red). The subpopulation of Stomatin$^+$ EVs is rich in AS-EVs (yellow). Bars: 10 μm. Data are presented as mean ± standard deviation (SD). $N = 3$ independent experiments, *p < 0.05, **p < 0.01, two-sided paired *t*-test. (For interpretation of the references to color in this figure legend, the reader is referred to the Web version of this article.)

and norepinephrine expression in plasma indicated that acute stress activates the HPA axis and the SNS by releasing these transmitters simultaneously (Zhang et al. 2021). However, although widely applied as stress indicators, corticosterone and norepinephrine levels are known to decrease to baseline levels after a short time window, but the biological effects on the organism might persist (Qing et al. 2020). Therefore, a sensitive yet stable stress indicator with direct functional associations is in demand to be established. Notably, considering chronic stress, complex stressors often depends on complicated yet dynamic factors which may influence the outcomes, such as the frequency, durability and strength of stressors (Hu et al. 2022; Sui et al. 2022), thus acute stress might be more suitable and convenient to support this pioneering work with EV biomarkers in psychological stress. However, it will still be necessary to verify or compare the EV biomarker in chronic stress in the future. Besides, the control group of restraint stress we used also suffered from FWD stress, even though the behavior experiments showed limited effects of FWD stress. The potential combined stress effects on EVs and Stomatin expression might exist. Further investigations including a large sample size will also need to be done, possibly in human samples, to strengthen and extend our findings.

EVs are membrane-bound nanoparticles providing a snapshot of dynamic physiological and pathological circumstances (Thietart and Rautou 2020). It is becoming increasingly clear that in response to a variety of stress conditions, EVs are released into circulation and continuously transmit messages for intercellular communication (Zhang et al. 2021). In this study, we used serial centrifugation to isolate EVs from the plasma, which holds a high fidelity to their natural state compared to other accessible isolation approaches (Khodayari et al. 2020). We further applied a variety of EV characterization methods based on the morphology, size, number, and expression of characteristic proteins according to the MISEV2018 guideline (Théry et al. 2018). The size distribution of the isolated EVs corresponds with the applied forces

of centrifugation for separating large EVs, with a putative origin from the plasma membrane (Mathieu et al. 2019). Therefore, these EVs possibly possess traceable surface markers from their parental cells that can also be easily isolated and examined, which thus provides advantages for diagnostic purposes (Cao et al. 2022). Stomatin, first isolated from human red blood cells (Hiebl-Dirschmied et al. 1991; Stewart et al. 1992; Wetzel et al. 2007), is a major component of lipid rafts of the plasma membrane (Lee et al. 2017b). The typical functions of stomatin are to control ion channels (Genetet et al. 2017; Moshourab et al. 2013) and modulate the organization of the actin cytoskeleton (An et al. 2019; Chen et al. 2013; Rungaldier et al. 2017). Studies in *C.elegans* have shown that the Stomatin domain-containing protein is required for touch receptor function (O'Hagan et al. 2005). Besides, touch-evoked pain caused by neuropathies is also impaired in *Stomatin-like protein 3* (*Stoml3*) mutant mice (Wetzel et al. 2007). These findings provide clues that Stomatin might be related to neurological alterations. Previous findings have also implied that Stomatin can promote membrane fusion putatively through EV trafficking (Lee et al. 2017a). Therefore, Stomatin is engaged in many biological processes and potentially in EV regulation. Indeed, the surface Stomatin has been identified by us on AS-EVs and the protein content alterations of AS-EVs existed in plasma for at least 24 h after the stress. How the changes are kept maintaining and when the effects will be vanished need further experiments. How Stomatin is regulated by psychological stress and its cellular origins will also be further investigated.

It is unequivocal that concentrations and composition of circulating EVs vary with disease conditions, with certain specificity for the ongoing pathological process (Szabo and Momen-Heravi 2017). Despite previous studies' consensus on evaluating psychological stress status by Heart Rate Variability and psychological assessment scale, a proper liquid biopsy test is absent (Park et al. 2022; Sgoifo et al. 2021). Due to this limit, we performed proteomic analysis of AS-EVs to guide data interpretation. The identified DEPs showed a response to stimulus and biological regulation functions. It is well known that stress stimuli can imply subsequent biological regulation (Hong et al. 2022), and inflammatory and metabolic adaptations occur after acute stress (Qing et al. 2020; Ray et al. 2017). Our results add to the current knowledge that EVs represent a critical complex platform where many of the regulatory proteins exist to be transported (Ray et al. 2017). Future studies will be performed to conduct functional experiments *in vitro* and *in vivo* to confirm the function of AS-EVs, particularly their regulatory effects on multiple cells and biological processes. Detailed research is also needed to identify the key component that mediates these effects. Based on these lines of evidence, the EV findings will contribute to a great extent to the psychological stress diagnosis and therapeutics.

Taken together, our study demonstrates that EVs are an important function-related liquid biopsy indicator that mediates circulation alterations impinged by acute psychological stress. These findings also support the idea that AS-associated EV-Stomatin can be used as a biomarker for potentially predicting stress responses and monitoring psychological status, which paves an avenue for implementing routine plasma EV-based theranostics in the clinic.

Funding

This work is supported by grants from the National Natural Science Foundation of China (82170988 to F.J., 81930025 to Y.J., 32101096 to X.Q., 32000974 to B.S.) and the China Postdoctoral Science Foundation (2019M663986 and BX20190380 to B.S.)

Institutional review board statement

The animal study protocol was approved by the Institutional Animal Care and Use Committee of the Fourth Military Medical University (protocol code 2014–073, date of approval 2014-9-6) for studies involving animals.

CRediT authorship contribution statement

Yuan Cao: Methodology, Formal analysis, Investigation, Data curation, Writing – review & editing, Visualization. **Si-Qi Ying:** Methodology, Formal analysis, Investigation, Data curation, Writing – original draft, preparation, Visualization. **Xin-Yu Qiu:** Resources, Funding acquisition. **Jia Guo:** Validation. **Chen Chen:** Resources. **Shi-Jie Li:** Software. **Geng Dou:** Methodology. **Chen-Xi Zheng:** Writing – review & editing. **Da Chen:** Software. **Ji-Yu Qiu:** Writing – review & editing. **Yan Jin:** Conceptualization, Supervision, Project administration, Funding acquisition. **Bing-Dong Sui:** Conceptualization, Methodology, Writing – review & editing, Supervision. **Fang Jin:** Conceptualization, Supervision, Project administration, Funding acquisition, All authors have read and agreed to the published version of the manuscript.

Declaration of competing interest

The authors declare no conflict of interest.

Data availability

Data will be made available on request.

Acknowledgments

We are grateful for the assistance of the National Experimental Teaching Demonstration Center for Basic Medicine (AMFU).

We thank PTM Biolabs Co., Ltd (Hangzhou, China) for help in analyzing the proteomic data.

Appendix A. Supplementary data

Supplementary data to this article can be found online at https://doi.org/10.1016/j.ynstr.2023.100513.

References

An, H., et al., 2019. Stomatin plays a suppressor role in non-small cell lung cancer metastasis. Chin. J. Cancer Res. 31 (6), 930–944.
Barel, E., et al., 2018. Gonadal hormones modulate the HPA-axis and the SNS in response to psychosocial stress. J. Neurosci. Res. 96 (8), 1388–1397.
Beninson, L.A., Fleshner, M., 2014. Exosomes: an emerging factor in stress-induced immunomodulation. Semin. Immunol. 26 (5), 394–401.
Bjørnetrø, T., et al., 2019. An experimental strategy unveiling exosomal microRNAs 486-5p, 181a-5p and 30d-5p from hypoxic tumour cells as circulating indicators of high-risk rectal cancer. J. Extracell. Vesicles 8 (1), 1567219.
Cai, W.P., et al., 2017. Relationship between cognitive emotion regulation, social support, resilience and acute stress responses in Chinese soldiers: exploring multiple mediation model. Psychiatr. Res. 256, 71–78.
Cao, Y., et al., 2022. Isolation and analysis of traceable and functionalized extracellular vesicles from the plasma and solid tissues. J Vis Exp 188.
Carroll, D., 2017. Genome editing: past, present, and future. Yale J. Biol. Med. 90 (4), 653–659.
Chen, J.C., et al., 2013. Up-regulation of stomatin expression by hypoxia and glucocorticoid stabilizes membrane-associated actin in alveolar epithelial cells. J. Cell Mol. Med. 17 (7), 863–872.
Coumans, F.A.W., et al., 2017. Methodological guidelines to study extracellular vesicles. Circ. Res. 120 (10), 1632–1648.
Doyle, L.M., Wang, M.Z., 2019. Overview of extracellular vesicles, their origin, composition, purpose, and methods for exosome isolation and analysis. Cells 8 (7).
Eden, E.R., Futter, C.E., 2021. Membrane trafficking: retrofusion as an escape route out of the endosome. Curr. Biol. 31 (17), R1037–r1040.
Genetet, S., et al., 2017. Stomatin modulates the activity of the anion exchanger 1 (AE1, SLC4A1). Sci. Rep. 7, 46170.
Hiebl-Dirschmied, C.M., et al., 1991. Cloning and nucleotide sequence of cDNA encoding human erythrocyte band 7 integral membrane protein. Biochim. Biophys. Acta 1090 (1), 123–124.
Hong, S.Z., et al., 2022. Norepinephrine potentiates and serotonin depresses visual cortical responses by transforming eligibility traces. Nat. Commun. 13 (1), 3202.
Hu, C.H., et al., 2022. Sympathetic neurostress drives osteoblastic exosomal MiR-21 transfer to disrupt bone homeostasis and promote osteopenia. Small Methods 6 (3), e2100763.
Hu, L., et al., 2014. A new stress model, a scream sound, alters learning and monoamine levels in rat brain. Physiol. Behav. 123, 105–113.

Huang, X., et al., 2015. Exosomal miR-1290 and miR-375 as prognostic markers in castration-resistant prostate cancer. Eur. Urol. 67 (1), 33–41.
Ji, R., et al., 2022. Association of self-leadership with acute stress responses and acute stress disorders in Chinese medics during the COVID-19 pandemic: a cross-sectional study. Front. Psychiatr. 13, 836950.
Khodayari, N., et al., 2020. Alpha-1 antitrypsin deficient individuals have circulating extracellular vesicles with profibrogenic cargo. Cell Commun. Signal. 18 (1), 140.
Labuschagne, I., et al., 2019. An introductory guide to conducting the trier social stress test. Neurosci. Biobehav. Rev. 107, 686–695.
Lee, J.H., et al., 2017a. Lipid raft-associated stomatin enhances cell fusion. Faseb. J. 31 (1), 47–59.
Lee, J.H., Lee, J.L., Kim, J.C., 2017b. Identification of recurrence-predictive indicators in stage I colorectal cancer: reply. World J. Surg. 41 (6), 1658–1659.
Li, X.J., et al., 2017. Xiaoyaosan exerts anxiolytic-like effects by down-regulating the TNF-α/JAK2-STAT3 pathway in the rat hippocampus. Sci. Rep. 7 (1), 353.
Marques-Feixa, L., et al., 2022. Secretory immunoglobulin A (s-IgA) reactivity to acute psychosocial stress in children and adolescents: the influence of pubertal development and history of maltreatment. Brain Behav. Immun. 103, 122–129.
Mathieu, M., et al., 2019. Specificities of secretion and uptake of exosomes and other extracellular vesicles for cell-to-cell communication. Nat. Cell Biol. 21 (1), 9–17.
Maugeri, M., et al., 2019. Linkage between endosomal escape of LNP-mRNA and loading into EVs for transport to other cells. Nat. Commun. 10 (1), 4333.
Moshourab, R.A., et al., 2013. Stomatin-domain protein interactions with acid-sensing ion channels modulate nociceptor mechanosensitivity. J. Physiol. 591 (22), 5555–5574.
O'Hagan, R., Chalfie, M., Goodman, M.B., 2005. The MEC-4 DEG/ENaC channel of Caenorhabditis elegans touch receptor neurons transduces mechanical signals. Nat. Neurosci. 8 (1), 43–50.
Obrist, P.A., 1976. Presidential Address, 1975. The cardiovascular-behavioral interaction–as it appears today. Psychophysiology 13 (2), 95–107.
Park, H.J., et al., 2022. Nurse evaluation of stress levels during CPR training with heart rate variability using smartwatches according to their personality: a prospective, observational study. PLoS One 17 (6), e0268928.
Pegtel, D.M., Gould, S.J., 2019. Exosomes. Annu. Rev. Biochem. 88, 487–514.
Pluchino, S., Smith, J.A., 2019. Explicating exosomes: reclassifying the rising stars of intercellular communication. Cell 177 (2), 225–227.
Pyter, L.M., et al., 2014. Contrasting mechanisms by which social isolation and restraint impair healing in male mice. Stress 17 (3), 256–265.
Qin, H.Y., et al., 2014. Impact of psychological stress on irritable bowel syndrome. World J. Gastroenterol. 20 (39), 14126–14131.
Qing, H., et al., 2020. Origin and function of stress-induced IL-6 in murine models. Cell 182 (2), 372–387 e14.
Ray, A., Gulati, K., Rai, N., 2017. Stress, anxiety, and immunomodulation: a pharmacological analysis. Vitam. Horm. 103, 1–25.
Rungaldier, S., et al., 2017. Structure-function analysis of human stomatin: a mutation study. PLoS One 12 (6), e0178646.
Sandi, C., Haller, J., 2015. Stress and the social brain: behavioural effects and neurobiological mechanisms. Nat. Rev. Neurosci. 16 (5), 290–304.
Sapolsky, R.M., Romero, L.M., Munck, A.U., 2000. How do glucocorticoids influence stress responses? Integrating permissive, suppressive, stimulatory, and preparative actions. Endocr. Rev. 21 (1), 55–89.
Segerstrom, S.C., Miller, G.E., 2004. Psychological stress and the human immune system: a meta-analytic study of 30 years of inquiry. Psychol. Bull. 130 (4), 601–630.
Sgoifo, A., et al., 2021. Psychobiological evidence of the stress resilience fostering properties of a cosmetic routine. Stress 24 (1), 53–63.
Shakirov, E.V., Chen, J.J., Shippen, D.E., 2022. Plant telomere biology: the green solution to the end-replication problem. Plant Cell 34 (7), 2492–2504..
Stewart, G.W., et al., 1992. Isolation of cDNA coding for an ubiquitous membrane protein deficient in high Na+, low K+ stomatocytic erythrocytes. Blood 79 (6), 1593–1601.
Sui, B., et al., 2022. Targeted inhibition of osteoclastogenesis reveals the pathogenesis and therapeutics of bone loss under sympathetic neurostress. Int. J. Oral Sci. 14 (1), 39.
Szabo, G., Momen-Heravi, F., 2017. Extracellular vesicles in liver disease and potential as biomarkers and therapeutic targets. Nat. Rev. Gastroenterol. Hepatol. 14 (8), 455–466.
Tan, K.H., et al., 2017. Extracellular vesicles yield predictive pre-eclampsia biomarkers. J. Extracell. Vesicles 6 (1), 1408390.
Théry, C., et al., 2018. Minimal information for studies of extracellular vesicles 2018 (MISEV2018): a position statement of the International Society for Extracellular Vesicles and update of the MISEV2014 guidelines. J. Extracell. Vesicles 7 (1), 1535750.
Thietart, S., Rautou, P.E., 2020. Extracellular vesicles as biomarkers in liver diseases: a clinician's point of view. J. Hepatol. 73 (6), 1507–1525.
Turner, A.I., et al., 2020. Psychological stress reactivity and future health and disease outcomes: a systematic review of prospective evidence. Psychoneuroendocrinology 114, 104599.
Wetzel, C., et al., 2007. A stomatin-domain protein essential for touch sensation in the mouse. Nature 445 (7124), 206–209.
Zeng, Z., et al., 2019. Efficacy of CoQ10 as supplementation for migraine: a meta-analysis. Acta Neurol. Scand. 139 (3), 284–293.
Zhang, Y., et al., 2008. Toll-like receptor 4 mediates chronic restraint stress-induced immune suppression. J. Neuroimmunol. 194 (1–2), 115–122.
Zhang, Z.Q., et al., 2021. Chronic stress promotes glioma cell proliferation via the PI3K/Akt signaling pathway. Oncol. Rep. 46 (3).
Zheng, C., et al., 2021. Apoptotic vesicles restore liver macrophage homeostasis to counteract type 2 diabetes. J. Extracell. Vesicles 10 (7), e12109.